Building block modeling technique: Application to ternary chalcogenide glasses g-Ge_{2}As_{4}Se_{4} and g-AsGe_{0.8}Se_{0.8}

B. Cai, X. Zhang, and D. A. Drabold

Phys. Rev. B **83**, 092202 — Published 21 March 2011

DOI: 10.1103/PhysRevB.83.092202

Building Block Modeling Technique: Application to Ternary Chalcogenide Glasses, g-$Ge_2As_4Se_4$ and g-$AsGe_{0.8}Se_{0.8}$

B. Cai
Dept. of Physics and Astronomy, Ohio University, Athens OH 45701, USA

X. Zhang
Dept. of Radiation Physics, University of Texas MD Anderson Cancer Center, Houston, TX 77030, USA
Dept. of Physics and Astronomy, Ohio University, Athens OH 45701, USA

D. A. Drabold
Dept. of Physics and Astronomy, Ohio University, Athens, OH 45701, USA
(Dated: Jan. 22, 2011)

Abstract: For some glasses, there are fundamental units, "Building Blocks" (BBs), that exist in both the liquid and glassy phases. In this paper, we introduce a systematic modeling technique based on the concept of BBs and obtain *ab-initio* models of g-$Ge_2As_4Se_4$ and g-$AsGe_{0.8}Se_{0.8}$. The total radial distribution function of g-$Ge_2As_4Se_4$ shows pleasing agreement with experimental data. The partial pair correlation functions are predicted for both g-$Ge_2As_4Se_4$ and g-$AsGe_{0.8}Se_{0.8}$. The coordination statistics indicate that the '8-N' rule is often violated in these two ternary chalcogenide glasses. The electronic density of states with inverse participation ratio analysis is also reported.

PACS numbers: 61.43.Bn, 61.43.Fs, 61.43.Dq
Keywords: Chalcogenide glasses; Building Block Method; Ge-As-Se alloy

Owing to promising optoelectronic and electronic features[1–3], chalcogenide glasses have drawn extensive attention during last decade. However, the lack of translational periodicity makes it hard to predict the microscopic structure of these glasses. Experimental results indicate that chemical order is broken and homopolar bonds are observed in chalcogenide glasses[4–6]. To further understand the topology and its role in determining optoelectronic and electronic properties, realistic atomistic models of these glasses are required. One possible way to obtain atomic models for glasses is the standard molecular dynamic (MD) 'melt and quench' method. This method seems to work when there are fundamental units existing in both liquid and glass. For simple BBs (involving only a few atoms), realistic models are obtained after a long liquid equilibration and a slow quench procedure. However, if the BBs are complex, such as the case in ternary alloys, it sometimes happens that the 'melt and quench' method fails to obtain the correct structure due to the limitation of short simulation times. If *a priori* information (such as chemical order, correct coordination number, etc.) is unknown for a target material, the 'melt and quench' technique usually starts with random initial configurations and the calculations may be extremely time-consuming for large systems. Also, very large cells may be required if the structural order is complex. Our earlier studies indicated that the 'melt and quench' method has difficulties in generating realistic atomic models of Ge-As-Se glasses (more details are discussed in Ref.7). Thus, in this case, it is of interest to develop a new modeling technique.

Since BBs play important roles in the 'melt and quench' method, we may first attempt to generate energetically reasonable (energy is minimum) BBs and then build a large cell from those BBs. This idea is based on two assumptions: (1) No dramatic changes in local order occur between the large system and small system; (2) BBs exist in these glasses and the correct chemical order can be obtained by a long *ab-inito* molecular dynamic simulation[7,8]. In this paper, we describe a systematic modeling technique to obtain BBs and then to achieve big models. By applying this method, we construct *ab-initio* models of g-$Ge_2As_4Se_4$ and g-

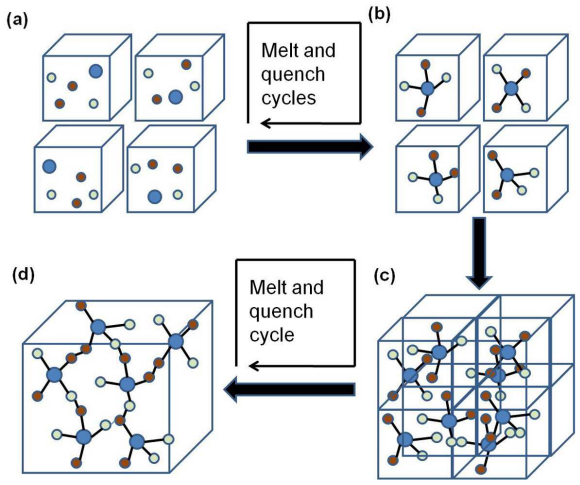

FIG. 1. (Color online) Flowchart for building block modeling method. (a) Atoms in sub-units cell with random initial positions. (b) Building blocks (BBs) are obtained after several 'melt and quench' cycles with unchanged minimum energy. (c) A large cell built, based on BBs. (d) Final models are obtained after one melt, quench/anneal cycle.

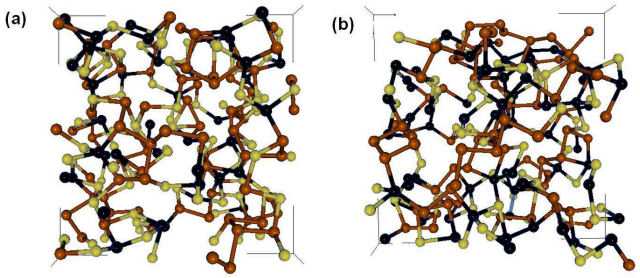

FIG. 2. (Color online) Atomic models for (a) 200-atom g-$Ge_2As_4Se_4$ and (b) 208-atom g-$AsGe_{0.8}Se_{0.8}$. Black (dark) atoms are Ge. Brown (grey) atoms are As. Green (light) atoms are Se.

$AsGe_{0.8}Se_{0.8}$. We compare the radial distribution function of g-$Ge_2As_4Se_4$ with experimental data and predict the partial pair correlation function for both g-$Ge_2As_4Se_4$ and g-$AsGe_{0.8}Se_{0.8}$. The electronic structures are studied through the electronic density of states. We found a 0.34 eV and a 0.38 eV electronic band gap for g-$Ge_2As_4Se_4$and g-$AsGe_{0.8}Se_{0.8}$ within the local density approximation (LDA).

We start our discussion by describing the MD procedures that are used to generate the atomic models. A flowchart to illustrate this method is given in Fig.1. A small number of atoms are randomly placed into a cubic box, we name the sub-unit cell, with the correct stoichiometry and experimental mass density. For g-$Ge_2As_4Se_4$, 25 atoms (5 Ge,10 Se and 10 As) are in each sub-unit cell with mass density 4.687g/cm^3 (lattice constant is 8.75 Å). For g-$AsGe_{0.8}Se_{0.8}$, 26 atoms (8 Ge,10 As and 8 Se) are in each sub-unit cell with mass density 4.459g/cm^3 (lattice constant is 9 Å). The sub-unit cells are then melted at 5000K for 1ps, equilibrated at 2000K for 15 ps, cooled over 1000K for 15 ps, annealed to 300K for 15 ps and quenched to 0K. These steps are repeated on the same sub-units for several cycles, until the minimum energy structures are unchanged. At this point, energetically optimized BBs are obtained. Then large unit cells are built from these BBs (200 atoms cells for g-$Ge_2As_4Se_4$ and 208 atoms cell for g-$AsGe_{0.8}Se_{0.8}$). We fix the temperature in the large cells at 1500K (above the melting point) for 7.5 ps, anneal to 300K and quench to 0K[7]. All the MD steps are done via the density functional quantum molecular dynamic method FIREBALL96 with local basis sets[9]. To further improve the chemical order and eliminate artifacts of the minimal basis, we annealed our models at 300K for 5 ps and quench to 0K with the Vienna Ab-initio Simulation Package (VASP)[10]–a plane wave density functional theory(DFT) code using the local density approximation (LDA). The final models are obtained after an energy relaxation. In all calculations, only the Γ point is used to sample the Brillouin zone. The electronic density of states (EDOS) is calculated with VASP.

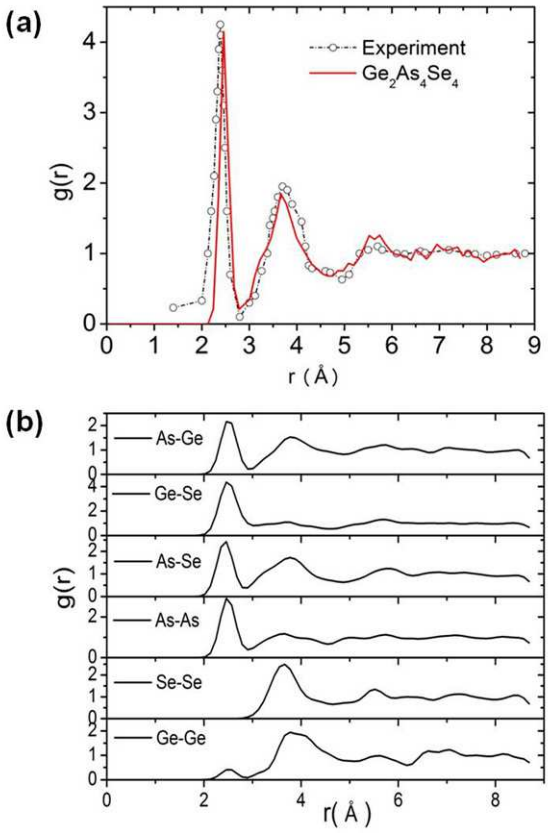

FIG. 3. (Color online) Radial distributions and partial pair correlation functions of g-$Ge_2As_4Se_4$. Experimental data is from Ref.11.

TABLE I. Mean bond length in g-$Ge_2As_4Se_4$ and comparison with Ref.11.

Bond type	Distance (Å)	Ref.11. (Å)
Ge-Ge	2.47	2.51±0.19
Ge-As	2.53	2.44±0.14
Ge-Se	2.53	2.48±0.15
As-As	2.50	2.41±0.07
As-Se	2.44	2.41±0.06

The final models are shown in Fig.2. We emphasize that there are no remaining correlations between the sub-unit cells in our final models. For g-$Ge_2As_4Se_4$, the radial distribution functions (RDF) and partial pair correlation functions (PPCF) are shown in Fig.3. The calculated total RDF indicates a sharp first peak at 2.47Å, a first minimum at 2.81Å and a broad second peak around 3.7Å. All the peak positions agree with experimental data from Ref.11, which implies that the building block techniques manage to obtain not only the correct local structure order but also a reasonable medium range order. The partial pair correlation functions for g-$Ge_2As_4Se_4$ are ploted in Fig.3(b). Ge-Se, As-Se, Ge-As and As-As all have a

strong first peak around 2.5Å which collectively produce the first peak in the total RDF. Se-Se homopolar-bonds are not observed in our models. We also noticed that As atoms bond with both Ge and Se atoms, which does not support the assumption that As-Ge bonds have low formation probability[12]. We list the averaged bond distance in Table I and they are close to the value predicted in Ref.11. Notice that Ref.11 predicted 2.41Å for As-As bond which is 3% lower than the standard value (2.49 Å for amorphous As[13] and 2.51 Å in rhombohedric As[14]), our results are actually closer to the standard value. For g-$AsGe_{0.8}Se_{0.8}$, the total RDF shows similar features to g-$Ge_2As_4Se_4$. With an increased concentration of Ge atoms, As-Se partial exhibits a weak first peak and a strong second peak; the number of Ge-Ge bonds are also increased. Again, Se-Se bonds are not observed.

The structural statistics for coordination and chemical order are computed for both models, and we report the result in Table II. One observation is that the '8-N' rule is not valid for our models. For g-$Ge_2As_4Se_4$, the majority of Ge, As and Se are four-fold, three-fold and two-fold, respectively. However, there is a significant fraction of three-fold Ge atoms and three-fold Se atoms in the system. For g-$AsGe_{0.8}Se_{0.8}$, the majority of Ge atoms are still four-fold and As atoms remain three-fold, while *most* Se atoms are three-fold. This may be due to a relatively large concentration of Ge atoms (compared with g-$Ge_2As_4Se_4$) and implies that g-$AsGe_{0.8}Se_{0.8}$ has a more rigid three dimensional network. These under-coordinated Ge atoms and over-coordinated Se atoms do not introduce mid-gap states or highly localized tail sates, so we do not interpret them as a defect. The average coordination $\langle r\rangle$ of our model is 2.93 for g-$Ge_2As_4Se_4$ and 3.08 for g-$AsGe_{0.8}Se_{0.8}$, which is different from the standard values proposed by Thorpe and Phillips (2.8 for g-$Ge_2As_4Se_4$ and 3.0 for g-$AsGe_{0.8}Se_{0.8}$) based on '8-N' constraints[15][16] (where the averaged coordination $\langle r\rangle$ is calculated as $\langle r\rangle$=$4X_{Ge}$+$3X_{As}$+$2X_{Se}$. X_{Ge}, X_{As} and X_{Se} are the concentration of Ge, As and Se atoms). When $\langle r\rangle$ is bigger than 2.8, it is believed that Ge-As-Se alloys form a three-dimensional rigid network due to the vulcanization or *cross-linking*. The difference here may imply that the constraint counting of Ge-As-Se alloys in this cross-linked 3-D region should be carefully reconsidered. Violations of the 8-N rule are well known in other chalcogenide systems[18].

Without any *a priori* information, the building-block method provided us reasonable models of g-$Ge_2As_4Se_4$ and g-$AsGe_{0.8}Se_{0.8}$. We should be clear that the building block technique is not new in modeling disordered materials. Amorphous Si_3N_4 models were made by Ouyang and co-authors through assembling a small number of fundamental building blocks[19]. However, the building blocks in our method were built purely from first principle calculation and the recipe is, in principle, perfectly general. Moreover, the final 'melt and quench' cycle for the large cell managed to maintain correct short range order, destroy the correlation of BBs and obtain credible medium range order at the same time. Considering the efficiency, since the large cells are constructed based on reasonable BBs, our simulation has a shorter computation time compared to the traditional method searching for optimum structures from random initials.

TABLE II. Coordination numbers and bond type analysis of computer generated g-$Ge_2As_4Se_4$ and g-$AsGe_{0.8}Se_{0.8}$.

Alloys	Element	Coordination					Bond type		
		5	4	3	2	Mean	Ge%	As%	Se%
g-$Ge_2As_4Se_4$	Ge	4	20	16	0	3.7	3	30	67
	As	0	6	74	0	3.1	18	45	37
	Se	0	1	30	49	2.4	52	48	0
g-$AsGe_{0.8}Se_{0.8}$	Ge	1	37	26	0	3.6	14	34	52
	As	0	8	70	2	3.1	32	49	19
	Se	0	0	39	25	2.6	72	28	0

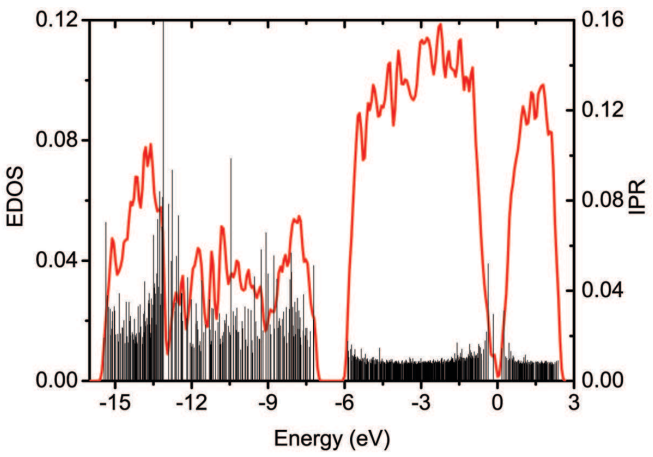

FIG. 4. (Color online) Electronic density of states (EDOS) and inverse participation ratio (IPR) for g-$Ge_2As_4Se_4$ model. The Fermi level is at 0 eV.

The electronic structure was analyzed through electronic density of states (EDOS) and inverse participation ratio (IPR). The IPR measures the localization for each eigenstate. For ideally localized states, IPR=1; for extended states, IPR=N^{-1}, where N is the number of atoms. (Details are discussed in Ref.17. All calculations are done via VASP.) The EDOS of g-$Ge_2As_4Se_4$ in Fig.4 indicates a 0.34 eV band gap and a mid-gap state. High IPR states are observed in the region from -15.5 eV to -6.5 eV and around the valence and conduction band edge. We then studied the localization by projecting the density of states onto different species. We could see from Fig.5, that Se atoms contribute to the region from -15.5eV to -13 eV, As atoms contribute to the region from -12.9 eV to -8.6 eV and Ge atoms contribute to the region from -8.6 eV to -7.2 eV. The eigenstates in the region from -5 eV to -1 eV are quite extended. The valence band tail states and conduction band tail states are tend to be localized on As and Ge

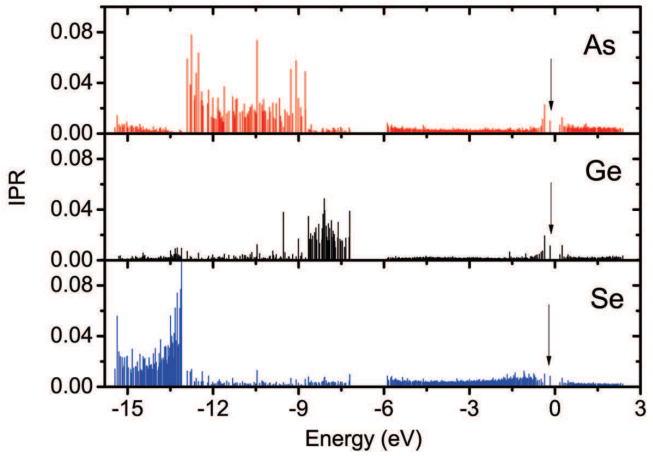

FIG. 5. (Color online) Projected IPR for g-$Ge_2As_4Se_4$ according to different species. The mid-gap state is marked by black arrow. The Fermi level is at 0 eV.

atoms. A further investigation shows that the gap states are mainly localized on over-coordinated (five-fold) Ge atoms and its neighbors. The valence tail state with highest IPR, is localized on a distorted site where three atoms (1 Ge, 1 As and 1 Se) form a triangle. We believe that the over-coordinated Ge site and the distorted triangle site would be eliminated through an extended annealing. The DOS of g-$AsGe_{0.8}Se_{0.8}$ exhibits a similar shape to g-$AsGe_{0.8}Se_{0.8}$ but with a 0.38 eV band gap and no mid-gap states. As atoms highly contribute to the valence and conduction band tail states. We should point out here that under-coordinated (3-fold) Ge atoms and over-coordinated (3-fold) Se atoms do not introduce localized states or mid-gap states, especially in g-$AsGe_{0.8}Se_{0.8}$ where most Se are 3-fold, which implies that they are not defects in the network. It is well known that the LDA method always under-estimates the magnitude of the band gap, so other techniques could be applied to get a better predication for the band gap[18].

To sum up, we introduced a BB modeling technique and applied it to obtain atomic models of g-$Ge_2As_4Se_4$ and g-$AsGe_{0.8}Se_{0.8}$. Both models predict reasonable RDFs and PPCFs, and the RDF of g-$Ge_2As_4Se_4$ shows reasonable agreement with experimental data. A significant fraction of over-coordinated Ge and under-coordinated Se are found in the system without introducing defect states in electronic structure, and we believe that these under-coordinated (3-fold) Ge and over-coordinated Se (3-fold) are not defects. This result may imply that the '8-N' rule is violated and the coordination constraint counting should be reconsidered in the rigid network region of Ge-As-Se alloys. We found a 0.34 eV band gap with a mid-gap state for g-$Ge_2As_4Se_4$ and 0.38 eV band gap for g-$AsGe_{0.8}Se_{0.8}$, which could be well under-estimate by LDA method.

This work was supported by the US NSF grant DMR 09-03225.

[1] R. W. Haisty and K. Krebs, J. Non-Cryst. Solids **1**, 427 (1969).
[2] P. J. Webber and J. A. Savage, J. Non-Cryst. Solids **20**, 271 (1976).
[3] T. T. Nang, M. Okuda, T. Matsushita, Phys. Rev. B **19**, 947 (1979).
[4] I. Petri, P. S. Salmon, H. E. Fischer, Phys. Rev. Lett. **84**, 2413 (2000).
[5] P. Hari, P. C. Taylor, W. A. King and W. C. LaCourse, J. Non-Cryst. Solids **198**, 736 (1996).
[6] P. S. Salmon, A. C. Barnes, R. A. Matin and G. J. Cuello, Phys. Rev. Lett. **96**, 235502 (2006).
[7] X. Zhang, PhD thesis, Ohio University, (2001).
[8] D. A. Drabold, Eur. Phys. J. B **68**, 1-21 (2009).
[9] O. F. Sankey, D. J. Niklewski, Phys. Rev. B **40**, 3979 (1989); J. P. Lewis, K. R. Glaesman, G. A. Voth, J. Fritsch, A. A. Demkov, J. Ortega and O.F. Sankey, Phys. Rev. B **64**, 195103 (2001); http://www.fireball-dft.org/web/fireballHome
[10] G. Kresse, J. Furthmuller, Phys. Rev. B **54**, 11169 (1996); http://cms.mpi.univie.ac.at/vasp/
[11] N. de la Rosa-Fox,L. Esquivias, P. Villares and R. Jimenez-Garay, Phys. Rev. B **33**, 4094 (1986).
[12] Z. U. Borisova, Glassy Semiconductors Plenum, New York (1981).
[13] G. N. Greaves and E. A. Davis, Philos. Mag. **29**, 1201 (1974).
[14] X. Wyckoff, in Crystal Structure (Wiley, New York, 1963).
[15] J. C. Phillips, J. Non-Cryst. Solids **34**, 153 (1979).
[16] M. F. Thorpe, J. Non-Cryst. Solids **57**, 355 (1983).
[17] D. A. Drabold, P. A. Fedders, Stefan Klemm, and O. F. Sankey, Phys. Rev. Lett. **67**, 2179 (1991); D. A. Drabold and P. A. Fedders, Phys. Rev. Lett. **60**, R721 (1999); D. A. Drabold, J. Noncryst. Solids **266**, 211 (2000); Raymond Atta-Fynn, Parthapratim Biswas, and D. A. Drabold, Phys. Rev. B **69**, 245204 (2004).
[18] B. Cai, D. A. Drabold and S. R. Elliott, Appl. Phys. Lett. **97**, 191908 (2010).
[19] L. Ouyang, W. Y. Ching, Phys. Rev. B **54**, 15594 (1996).
[20] B. Effey, R. L. Cappelletti, Phys. Rev. B **59**, 4119 (1999).